Periodic Analysis of MR-Safe Transmission Lines

Richard R. A. Syms, *Senior Member, IEEE*, Laszlo Solymar, and Ian R. Young

(Invited Paper)

***Abstract*—In this paper, a theoretical analysis is presented of transmission lines that are periodically interrupted by isolation transformers. Such lines have application as safe interconnects in MRI with internal coils, where the transformers act to block common-mode signals excited by the transmitter while passing differential-mode signals from a detector. The dispersion characteristics are derived, and it is shown that the line is a form of metamaterial supporting magneto-inductive (MI) waves. Propagation can take place in a series of bands, each close to one of the standing wave resonances of an isolated segment. However, it is shown that additional series capacitors are required to implement the protection strategy correctly and the line then operates on a low-frequency lumped-element MI band. Lines operating at 63.8 MHz frequency are constructed using coaxial cables and printed circuit board transformers, and the existence of multiple propagating bands is confirmed.**

***Index Terms*—MRI, magneto-inductive (MI) wave, metamaterial, periodic structure.**

I. Introduction

PERIODIC structures have long been of interest in electrical engineering, and many different arrangements of reactive elements have been used as filters and slow-wave circuits [1], [2]. Renewed interest in periodic electrical structures was sparked by the realization they can act as artificial media with negative permittivity, permeability, or refractive index [3]–[5]. Such has been the explosion of activity that "metamaterials" are now an entire field [6], [7].

Although most researchers concentrate on exploitation of negative parameters, other important applications exist. For example, it is well known that the electric field associated with the magnetic field of the RF transmitter used in MRI may cause resonant heating in conductors inserted into body tissues [8], [9]. The problem predominantly occurs in linear conductors arranged parallel to the electric field when the length of any potentially resonant section approaches half a wavelength, as shown in Fig. 1. Since the average relative dielectric constant of human tissue at the frequency $f = 63.8$ MHz used for ^{1}H MRI at 1.5 T field is $\varepsilon_{r\_\mathrm{tissue}} \approx 77$, the resonant length of an immersed cable may be as small as $d = c/(2f\sqrt{\varepsilon_{r\_\mathrm{tissue}}}) \approx 27$ cm [10], [11]. This length increases if the conductor has a cladding with a low dielectric constant, but resonant heating can occur for typical body insertion distances, and may be dangerous when imaging with internal coils.

Manuscript received June 5, 2009; revised August 28, 2009. First published October 23, 2009; current version published April 7, 2010. This work was supported by the Engineering and Physical Sciences Research Council under Grant EP/D032687/1 "Magneto-inductive ring waveguide detector."

The authors are with the Department of Electrical and Electronic Engineering, Imperial College London, London, SW7 2AZ, U.K. (e-mail: r.syms@imperial.ac.uk; laszlo.solymar@hertford.ox.ac.uk; youngimar@aol.com).

Digital Object Identifier 10.1109/JSTQE.2009.2032782

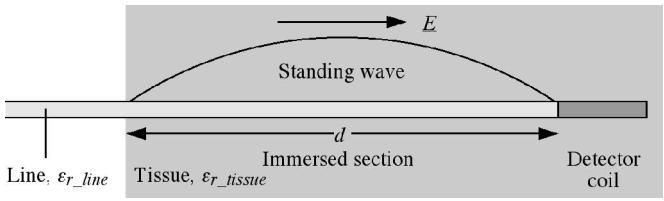

Fig. 1. Excitation of an external resonance on an immersed, conducting probe in internal MRI.

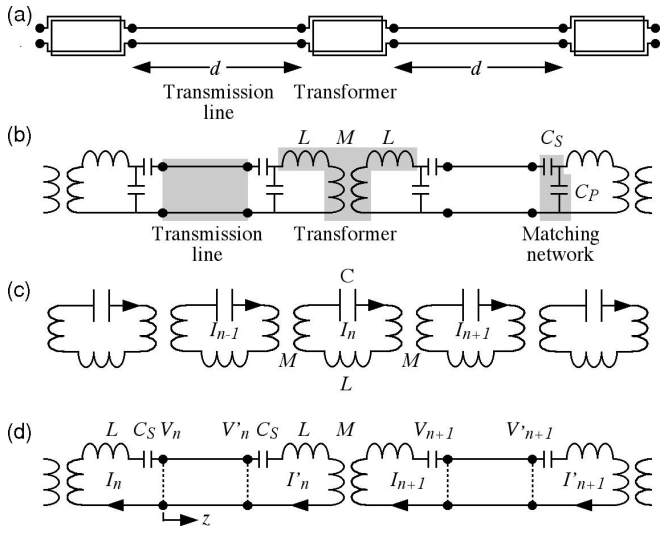

Fig. 2. (a) Arrangement and (b) equivalent circuit of MR-safe transmission line, including matching network, (c) MI waveguide and (d) equivalent circuit for analysis.

One early solution for cables involved coaxial chokes [11], [12], while a more recent solution is based on subdivision of the line using transformers [13], [14]. Fig. 2(a) shows a transformer-coupled MR-safe line and Fig. 2(b) shows its equivalent circuit. Here, additional series and parallel capacitors C_S and C_P are provided to assist impedance matching. This arrangement can pass differential-mode output signals from a detector when establishing an effective barrier against electrically induced common-mode signals. The MRI application requires air-cored transformers, and figure-of-eight windings that can reject external time-varying magnetic fields have also been developed [15].

Transformer coupling also provides a solution to the alternative problem of providing electrical isolation against common-mode leakage currents. Generally, only a few transformers are used; however, an infinite, regularly subdivided transmission line clearly requires a full periodic analysis.

1-D and 2-D arrangements of transmission lines with periodic loads have been extensively studied by Caloz [16]–[18] and Eleftheriades [19]–[21], who each showed that a variety of behavior, including propagating bands supporting both forward and backward waves, could arise. However, the MR-safe transmission line achieves its effect using inductive coupling, and such structures have received little attention so far. In this respect, the MR-safe line is more closely analogous to magneto-inductive (MI) waveguides, which are based on magnetically coupled chains of *L–C* resonators, as shown in Fig. 2(c) [22]–[24]. MI waves have been observed in other metamaterials, such as "metasolenoids" [25], [26] and "Swiss rolls" [27], and have applications in delay lines [28], phase shifters [29], and imaging lenses [30], [31]. Transmission of MR images through rigid "Swiss rolls" has also been demonstrated [32]. Magnetically coupled media are the subjects of several recent reviews (see, e.g., [7], [33], and [34]).

Understanding of MR-safe transmission lines is embryonic, and their periodic nature has been entirely neglected so far [13]–[15]. The aim of this paper is to provide a full periodic analysis in a metamaterial context using the simplified circuit of Fig. 2(d), which omits the parallel capacitors C_P. In Section II, a suitable theory is developed by extending an analysis for purely transformer-coupled lines, which omitted both C_P and the series capacitors C_S [35]. The dispersion characteristics of lossless lines are obtained, and the existence of multiple propagating bands is predicted. In Section III, numerical examples are presented, and it is shown that the capacitors C_S are essential for operation at suitable frequencies, while impedance matching may be carried out inductively. Verification is provided in Section IV using coaxial lines coupled by printed circuit board (PBC) transformers, and the existence of multiple bands is confirmed. Conclusions are presented in Section V.

II. Theoretical Analysis

In this section, we provide a theoretical framework for MR-safe transmission lines using a Bloch-wave solution of the recurrence relations to find the dispersion characteristic and the characteristic impedance.

A. Geometry

Fig. 2(d) shows the assumed geometry, which consists of identical sections of line, coupled together by air-cored transformers and series capacitors [13], [14]. Provided capacitive coupling between the transformer windings is low, the transformers allow propagation of differential-mode signals from an RF detector, but block common-mode signals excited directly by the MR transmitter. Common-mode signals may still resonate, but now only at higher frequencies defined by the shorter length d.

The discussion in [13] and [14] is specific concerning the need to block externally excited common-mode signals. The alternative of a composite right-/left-handed (CRLH) or backward-wave transmission line in the conventional arrangement would certainly provide the required bandpass characteristics for internal signals, but no protection against heating by external waves due to the lack of transformer isolation between sections.

Here, the use of inductive coupling to connect a set of line segments suggests that the arrangement will be similar to an MI waveguide, which has a bandpass characteristic [22], [23]. However, replacement of *L–C* resonators with sections of transmission line (which may be multiply resonant) might be expected to introduce additional propagating bands.

B. Recurrence Relations

We assume that the line sections have length d, impedance Z_0, and phase velocity v_P. If we define nodal voltages V_n and V_n' and currents I_n and I_n' at the two ends of the nth section, as shown in Fig. 2(d), Kirchhoff's laws give

$$\begin{aligned} V_n &= -\mathrm{j}(\omega L - 1/\omega C_S) I_n - \mathrm{j}\omega M I'_{n-1} \\ V'_n &= +\mathrm{j}(\omega L - 1/\omega C_S) I'_n + \mathrm{j}\omega M I_{n+1}. \end{aligned} \tag{1}$$

Since there are likely to be standing waves in the transmission line sections, we assume solutions for the voltages and currents in the form of pairs of counterpropagating waves as

$$\begin{aligned} V_n &= \exp(-\mathrm{j}n\phi)[V^+ + V^-] \\ V'_n &= \exp(-\mathrm{j}n\phi)[V^+ \exp(-\mathrm{j}kd) + V^- \exp(+\mathrm{j}kd)] \\ I_n &= \exp(-\mathrm{j}n\phi)\frac{[V^+ - V^-]}{Z_0} \\ I'_n &= \exp(-\mathrm{j}n\phi)\frac{[V^+ \exp(-\mathrm{j}kd) - V^- \exp(+\mathrm{j}kd)]}{Z_0} \end{aligned} \tag{2}$$

where V^+ and V^- are the amplitudes of the two waves, $k = \omega/v_{ph}$ is the propagation constant, and ϕ is the phase shift per section.

C. Dispersion Equation

Substituting (2) into (1) and collecting terms, we obtain the following simultaneous equations:

$$\begin{aligned} &V^+\{Z_0 + \mathrm{j}(\omega L - 1/\omega C_S) + \mathrm{j}\omega M \exp(-\mathrm{j}kd)\exp(+\mathrm{j}\phi)\} \\ &\quad + V^-\{Z_0 - \mathrm{j}(\omega L - 1/\omega C_S) \\ &\qquad - \mathrm{j}\omega M \exp(+\mathrm{j}kd)\exp(+\mathrm{j}\phi)\} = 0 \\ &V^+\{[Z_0 - \mathrm{j}(\omega L - 1/\omega C_S)]\exp(-\mathrm{j}kd) - \mathrm{j}\omega M \exp(-\mathrm{j}\phi)\} \\ &\quad + V^-\{[Z_0 + \mathrm{j}(\omega L - 1/\omega C_S)]\exp(+\mathrm{j}kd) \\ &\qquad + \mathrm{j}\omega M \exp(-\mathrm{j}\phi)\} = 0. \end{aligned} \tag{3}$$

Eliminating either of the voltage amplitudes, we then obtain the dispersion equation

$$\begin{aligned} &\{Z_0^2 - [(\omega L - 1/\omega C_S)^2 - \omega^2 M^2]\}\sin(kd) \\ &\quad + 2Z_0\{(\omega L - 1/\omega C_S)\cos(kd) + \omega M \cos(\phi)\} = 0. \end{aligned} \tag{4}$$

We now introduce some notation to allow (4) to be recast in normalized form. The resonances of order ν for a short-circuited line of length d are defined by $k_\nu d = \nu\pi$, and the corresponding angular resonant frequencies are given by $\omega_\nu = \nu\pi v_P/d$. Hence, $kd = \pi w$, where $w = \omega/\omega_1$ is a normalized

frequency and ω_1 is the lowest line resonance. The resonant frequency due to the lumped-element components alone is $\omega_S = 1/(LC_S)^{1/2}$, and we characterize its value using the parameter $s = \omega_1/\omega_S$. The modulus of the impedance of the inductance $|\mathrm{j}\omega L|$ and the line Z_0 are equal at an angular frequency ω_M when $L\omega_M = Z_0$, and we may characterize the value of ω_M using the parameter $m = \omega_1/\omega_M$. Finally, the effectiveness of the transformer may be described by a ratio $\alpha = M/L$. This parameter is related to the coupling coefficient $\kappa = 2M/L$ used in the analysis of MI waves [19], the absence of the factor of 2 arising here from division of the series inductance into two. With this notation, (4) can be rewritten as follows:

$$\{1 - w^2m^2[(1 - 1/w^2s^2)^2 - \alpha^2]\}\sin(\pi w) + 2wm\{(1 - 1/w^2s^2)\cos(\pi w) + \alpha\cos(\phi)\} = 0. \quad (5)$$

To see the implications of (5), we first assume that there is no series capacitance C_S (so that s becomes infinite). In this case, the dispersion equation simplifies to

$$\{1 - w^2m^2(1 - \alpha^2)\}\sin(\pi w) + 2wm\{\cos(\pi w) + \alpha\cos(\phi)\} = 0. \quad (6)$$

Similarly, for an isolated line segment ($\alpha = 0$), we get

$$(1 - w^2m^2)\sin(\pi w) + 2wm\cos(\pi w) = 0. \quad (7)$$

D. Impedance

It is also of interest to know the characteristic impedance of the line. Following [7], we determine this quantity by asking what lumped impedance Z_T could be inserted into the nth element of a finite line near the final inductor, which might compensate for the absence of a missing $(n+1)$th element. This impedance is most easily inserted via a further transformer. At the last element, the second equation of (3) then modifies to

$$V_n' = \{\mathrm{j}(\omega L - 1/\omega C_S) + Z_T\}I_n'. \quad (8)$$

Comparison with the second equation of (3) then shows that the lumped element termination will provide the appearance of an infinite line if

$$Z_T = \mathrm{j}\omega M\left(\frac{I_{n+1}}{I_n'}\right) = \mathrm{j}\omega M\left(\frac{I_n}{I_n'}\right)\exp(-\mathrm{j}\phi) \quad (9)$$

where I_n and I_n' may be obtained using (2) and (3), so that

$$I_n/I_n' = \{Z_0 + \omega M\sin(kd)\exp(\mathrm{j}\phi)\} / \{Z_0\cos(kd) - (\omega L - 1/\omega C_S)\sin(kd)\}. \quad (10)$$

Finally, using (4), (9), and (10), the impedance may be determined as a function of ω or ϕ.

The aforementioned theory neglects losses, which will arise primarily in the coupling transformers and the coaxial cable. Their effect will be to introduce propagation loss and alter characteristic impedance. However, for low losses, the theory should still provide a reasonable model.

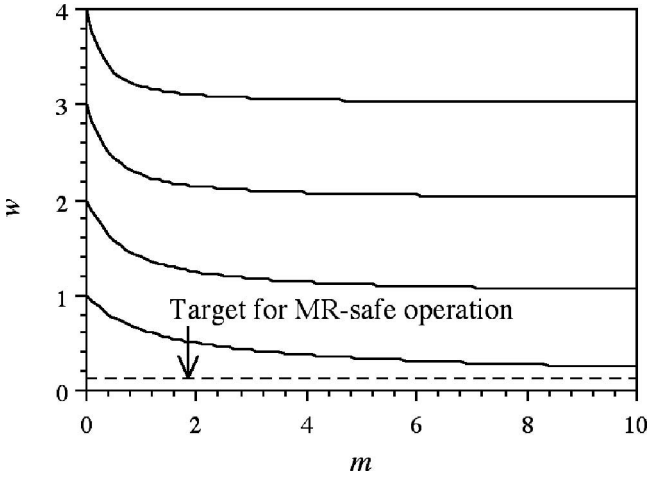

Fig. 3. Theoretical variation of the first four normalized resonant frequencies of an isolated segment with the normalized parameter $m = \omega_1/\omega_M$, assuming that the normalized parameter $s = \omega_1/\omega_S$ is infinite so that series capacitors may be neglected.

III. Numerical Examples

We now present some numerical examples, considering the system first without and then with the additional series capacitors C_S. To place the results into context, we first consider what value of normalized frequency should be chosen to operate the line in an MR-safe mode.

A. MR-Safe Operation

From Section I, we know that when the first external resonance of a line immersed in a medium with a dielectric constant, $\varepsilon_{r\_\mathrm{tissue}}$ occurs. However, the line itself has a much lower internal dielectric constant (e.g., $\varepsilon_{r\_\mathrm{line}} = 2$ for a polytetrafluoroethylene (PTFE) dielectric fill). Its first internal resonance occurs when $d = c/(2f_1\sqrt{\varepsilon_{r\_\mathrm{line}}})$. Assuming that the line is just short enough to prevent external resonances, this condition corresponds to a normalized frequency of $f/f_1 \approx \sqrt{(\varepsilon_{r\_\mathrm{line}}/\varepsilon_{r\_\mathrm{tissue}})} \approx \sqrt{(2/77)} \approx 1/6$. To guarantee safety, we might therefore require a slightly less value, say 1/7.

B. System Without Series Capacitor

Fig. 3 shows the variation with *m* of the first four normalized resonant frequencies, as predicted by (7). For $m = 0$ (when *L* is 0), we clearly obtain the resonances of a short circuit line of length *d* ($w = 1, 2, \ldots$). As the value of *m* increases, the solutions are each dragged down to lower frequency. However, the MR-safe function requires operation near the dashed line condition $w \approx 1/7$.

Although the resonances of an isolated segment are only indicative of broader frequency bands in a coupled system, we can immediately see that large values of *m* will be required. Consequently, large inductors will be needed, which may have undesirable consequences such as sensitivity to external fields.

Fig. 4 now shows the ω–k variation for a coupled system, as predicted by (6), assuming a typical value of $m = 7$. The thick lines show the result for $\alpha = 1$ (corresponding to a perfect

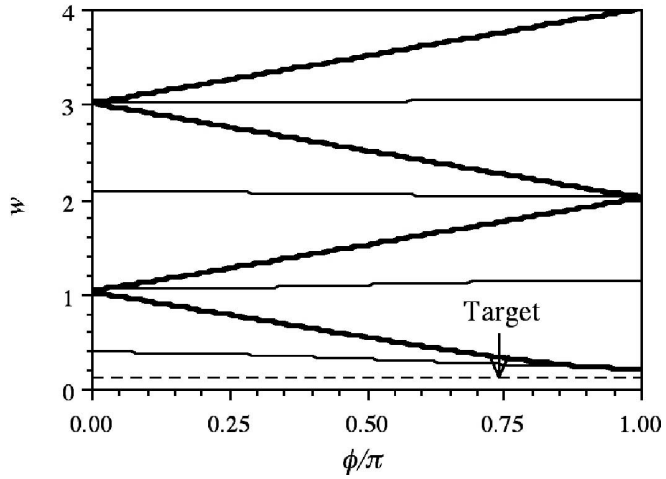

Fig. 4. Theoretical dispersion characteristics for the lowest bands of a transformer coupled line for $m = 7$, and $\alpha = M/L = 1$ (thick lines) and $\alpha = 0.5$ (thin lines), assuming that s is infinite.

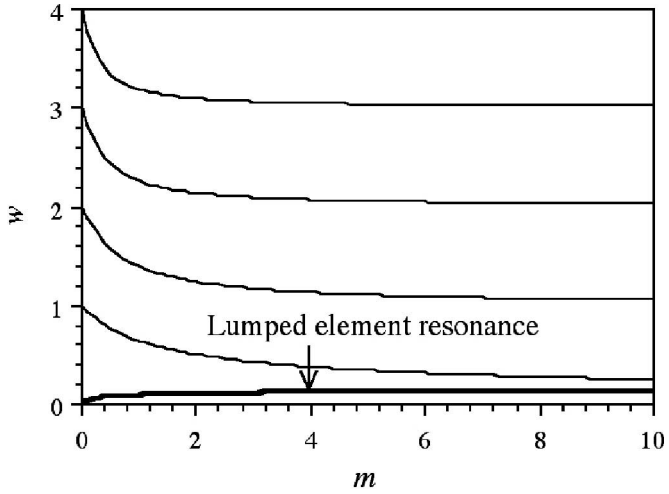

Fig. 5. Theoretical variation of the first four normalized resonant frequencies of an isolated line segment with m, assuming that $s = 7$.

transformer), and the thin lines for $\alpha = 0.5$ (a typical value for an air-cored transformer).

In each case, the discrete resonances of the isolated segments have split into bands, which alternate in type from forward wave to backward wave. These bands are clearly similar to, but not precisely the same as, MI bands and, for clarity, we term them transmission-line MI bands. For $\alpha = 1$, the widths of the bands are very large, occupying almost the whole frequency range between neighboring isolated-line resonances. However, for $\alpha = 0.5$, the bandwidths are significantly reduced. In each case, the closest approach to the MR-safe operating condition is in the lowest band near $\phi = \pi$, but it is not possible to reach it.

C. System With Series Capacitor

We now consider the effect of the series capacitor C_S. Fig. 5 shows the variation with m of the resonances of an isolated line segment, assuming that $s = 7$.

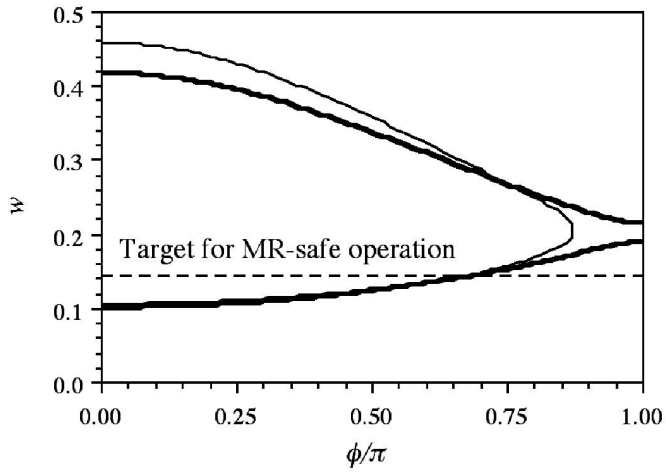

Fig. 6. Theoretical dispersion characteristics for a transformer coupled line for $m = 7$ and $s = 7$, and $\alpha = 0.5$ (thick lines) and $\alpha = 0.6$ (thin lines).

Comparison with Fig. 3 shows that the effect of C_S is to insert an additional low-frequency resonance, whose position can be adjusted to the target frequency by the value of s, independent of the precise value of m. The value of this resonance tends to $1/s$ (here, 1/7) when m is large.

Fig. 6 shows the ω–k variation for a complete coupled system predicted by (5), now assuming that $m = 7$ and $s = 7$. Two sets of data are shown, concentrating on the important frequency range below $w = 1$. The thick lines show results obtained when $\alpha = 0.5$. Here, the effect of coupling is to broaden each of the two resonances into bands. The lowest band corresponds to a lumped-element MI wave and now passes through the target frequency range easily. The values of m and s mainly determine the center frequencies of the bands, while the coupling coefficient α determines their widths. For slightly larger coupling (for example, $\alpha = 0.6$), the bands can be made to merge, as shown by the thin lines.

Since the MR-safe function is satisfied by the lumped-element MI wave (rather than its transmission-line equivalent), it is worth considering if this aspect emerges naturally from the analysis. We note that MR-safe operation requires $w \ll 1$. In this case, (5) approximates to

$$(1 - 1/w^2 s^2) + \alpha \cos(\phi) = 0. \tag{11}$$

Comparison with the literature [7] shows that indeed the dispersion characteristic of an MI wave, provided the coupling coefficient, is taken as α rather than κ.

In this branch, $I_n/I'_n \approx 1$ and (9) reduces to $Z_C = \mathrm{j}\omega M \exp(-\mathrm{j}\phi)$, the impedance of an MI waveguide [7]. At midband ($\phi = \pi/2$, where $\exp(-\mathrm{j}\phi) = -\mathrm{j}$), the characteristic impedance therefore has the positive real value $Z_C = \omega M$. Consequently, impedance matching can be carried out by an appropriate choice of M after the resonant frequency has been set by C_S and L.

Using normalized notation, we may rewrite this result as $Z_C = Z_0(m\alpha/s)$. The line impedance will therefore equal Z_0 if $m\alpha = s$, without the need for further measures. For $\alpha = 1$, we then require $m = s$, as was chosen here. However, since a larger

value of *m* (and hence, a larger inductance) may be needed when α is smaller, it may be simpler to accept a reduced value of Z_C and carry out impedance matching at the input and output of the line using transformers.

Finally, we note that we have investigated the effect of the parallel capacitors C_P used in [13] and [14]. We used exactly the same approach of periodic analysis followed by numerical evaluation of dispersion characteristics. The effect is, not unnaturally, to complicate the dispersion characteristics still more. Further resonances are introduced in isolated segments and further bands in transformer-coupled lines. However, the parallel capacitors do allow further design freedom to achieve impedance matching.

IV. Experimental Verification

To verify the concepts of the previous section, experiments were carried out using prototype MR-safe lines constructed from coaxial cable and PCB inductors. The elements themselves were designed to demonstrate physical principles and were not optimized for internal MR operation. The experiments were conducted in air rather than in a surrounding medium with a high dielectric constant, since the external surround does not affect transmission inside the line, and our purpose here is to explain signal propagation characteristics. While the surrounding does affect external waves, their excitation requires a powerful external transmitter, such as the TX coil in an MRI scanner. Unfortunately, access to a local clinical scanner simply to carry out such tests is currently unjustifiable due to patient loading. However, lines were designed to operate at 63.8 MHz, the frequency for ^{1}H MRI in a 1.5 T magnetic field.

A. Experimental Arrangement

Characterization was performed using an Agilent E5061A electronic network analyzer. Lines were constructed using coaxial cable terminated with single-loop inductors formed on FR-4 PCBs. The cable was a miniature (2.5 mm diameter) 50 Ω type (Nexans RG 174), with a propagation loss of $\approx 1.35 \times 10^{-3} \times f$ dB/m. The segment length *d* was chosen as 20 cm, shorter than the estimated minimum safe length (in contrast to the 37.5 cm used in [13] and [14], and 68.5 cm in [35], which are both too long). The lowest order internal resonance of a short-circuited segment was obtained by using a weak inductive probe as $f_1 = \omega_1/2\pi = 495$ MHz, suggesting an internal dielectric constant of $\varepsilon_{r\_\mathrm{line}} = 2.3$, in agreement with the manufacturer's data of 2.25 (for a polyethylene dielectric fill).

PCB inductors were formed from single turns of 0.5-mm-wide Cu track measuring 8 mm × 64 mm. Parameters were determined by making single inductors resonant using surface-mount capacitors. Capacitor values were assumed to be as quoted by the manufacturer, since these are reasonably accurate at the low RFs of MRI signals. The inductance was determined from the resonant frequency and capacitance as 115 nH, and the frequency $f_M = Z_0/2\pi L$ and frequency ratio $m = f_M/f_1$ from the inductance as 69.2 MHz and 7.15, respectively. The value of *m* is close to the value of 7 assumed in Section III. The *Q*-factor was determined from the bandpass characteristic of the resonant element as 91 at 100 MHz. The low *Q*-factor arises from the low operating frequency and the relatively poor design of the inductor (a single turn of a long, thin rectangular loop) used to mimic the transformer shape required in a real MR-safe application.

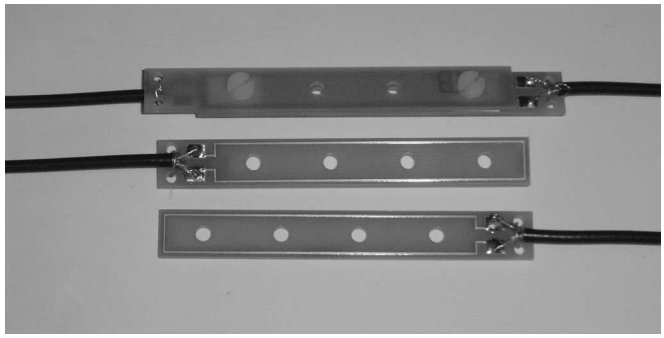

Fig. 7. Arrangement of experimental MR-safe lines based on segments of coaxial cable linked by PCB-based air-cored transformers.

The inductors were bolted together to form air-cored transformers using thin dielectric spacers to reduce capacitive coupling. The coupling coefficient α was determined from the frequency splitting obtained when two similar resonant elements were attached and variable using in the range 0.45–0.65, depending on the spacer thickness. Transmission line elements were constructed by attaching inductors to coaxial cables, as shown in Fig. 7, and the input and output coupling was carried out using similar inductors. Lines were constructed with up to eight elements, giving an overall cable length of just over 2 m. This length is realistic for *in vivo* human MRI with an internal RF detector coil.

The segmented MR-safe cable presented here was designed for ease of experimentation. The air-cored transformers were arranged to be repetitively separable, and hence are both oversize and rigid. Similarly, oversize coaxial cable was used to retain sufficient strength at soldered joints. In practice, thin-film transformers and subminiature coaxial cable would be used, as in [13] and [14]. These elements would then require the mechanical support of a catheter to allow insertion into (for example) an artery for vascular imaging.

B. MR-Safe Cables

First, it was verified that it was not possible to obtain propagation at 63.8 MHz frequency without using the series capacitors C_S, since the lowest order resonant frequency of an isolated segment was then only 145 MHz. The lines were therefore loaded with capacitors, and it was found that the lowest order resonance of an isolated segment could be reduced to 63.8 MHz when $C_S = 45$ pF. The lumped element resonance $f_S = 1/2\pi\sqrt{(LC_S)}$ and the frequency ratio $s = f_1/f_s$ were then established as 70 MHz and 7.07, respectively. The value of *s* is again close to the value of 7, previously assumed in Section III.

Fig. 8 shows the frequency variation of the scattering parameter S_{21} for lines with $N = 1$ and $N = 8$ segments. In the former case, the lumped element resonance and the

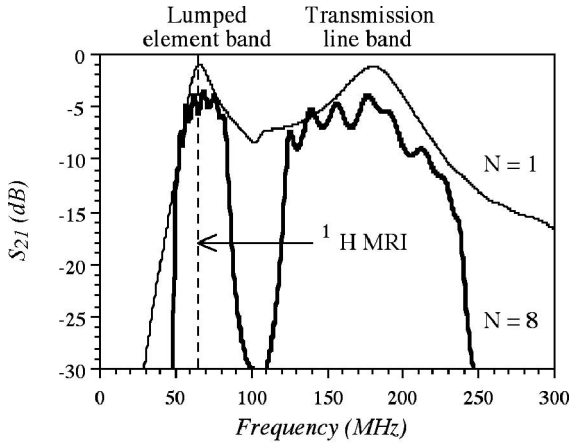

Fig. 8. Experimental frequency variation of the scattering parameter S_{21} for MR-safe lines with $N = 1$ and $N = 8$ sections.

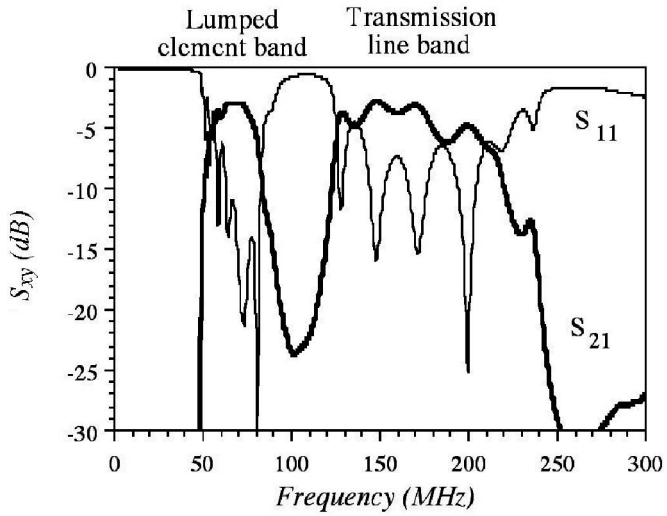

Fig. 9. Experimental frequency variation of the scattering parameters S_{21} and S_{11} for MR-safe lines with $N = 8$ sections and optimized input and output coupling.

lowest order transmission line resonance may be clearly identified at 63.8 and 180 MHz, respectively. In the latter case, the isolated resonances have each separated into bands, with ripples in the passband arising from end reflections. The lower, lumped-element MI propagation band is centered on a 63.8 MHz frequency, and is relatively narrow, as shown in Fig. 6, while the higher transmission-line band is considerably wider. In each case, transmission losses are lowest at the band center and rise rapidly at the band edges. Other higher order transmission line bands were observed using lines with longer line segments.

Fig. 9 shows the frequency variation of S_{21} and S_{11} obtained after adjustment of the spacer thickness in the input and output coupling transformers to improve impedance matching. The passband ripple has been substantially eliminated, and the reflection near the band center has been reduced below -10 dB, to a level suitable for operation in a commercial MRI scanner. The insertion loss at 63.8 MHz is around 3 dB, which would again be suitable for practical operation without significant signal loss.

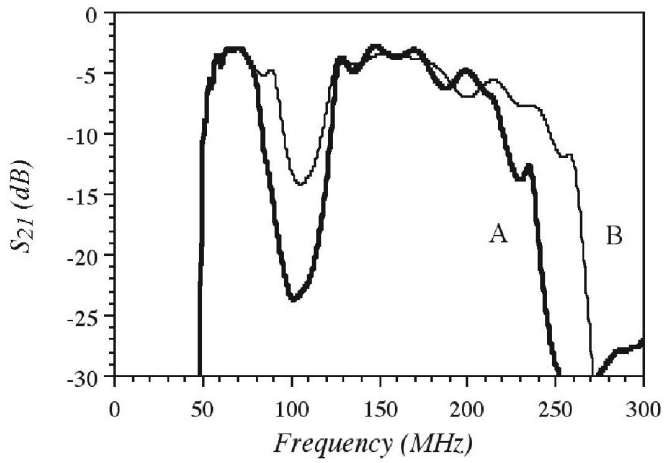

Fig. 10. Experimental frequency variation of the scattering parameter S_{21} for MR-safe lines with $N = 8$ sections and slightly different coupling coefficients α obtained by variations in transformer spacer thickness.

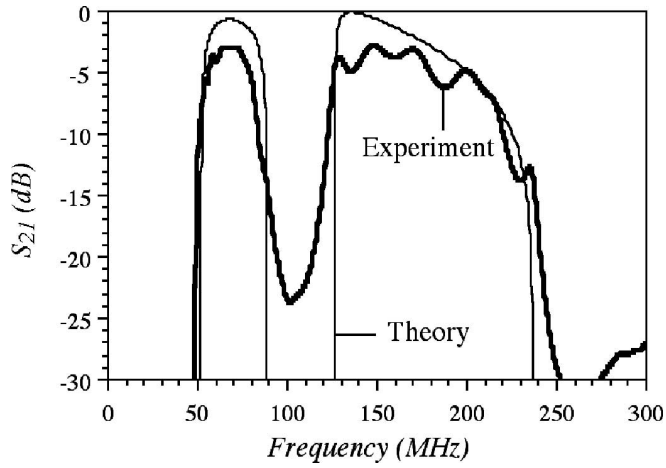

Fig. 11. Comparison between the experimental results of Fig. 9 and the predictions of simple theory.

Finally, Fig. 10 shows two frequency variations of S_{21} (labeled A and B) obtained for two slightly different spacer thicknesses, illustrating how the width of the passbands may be adjusted by the mutual coupling in the transformer. As expected from Fig. 6, there is little change at the bottom of the lumped element band. There are larger changes at the top of this band and at the top of the transmission line band, which tend to widen both bands and reduce the interband gap.

C. Comparison With Theory

Although losses have been omitted from the theoretical model and are inevitably present in the experiment, it is still useful to make an elementary comparison between the two. At least this will establish whether the propagation bands can be correctly determined by simple theory. Furthermore, in a lowloss system, multiple reflections caused by mismatch at input and output will lead to etalon effects. Here, we ignore losses and multiple reflections, and simply estimate transmission as $S_{21} = (1 - R_{\rm in}) \times (1 - R_{\rm out})$. $R_{\rm in}$ and $R_{\rm out}$ are the power reflection coefficients

at the input and output junctions between the MR-safe cable and the coaxial cable, and are determined from the appropriate impedances. Fig. 11 compares the experimental data of Fig. 9 with the frequency variation of S_{21} predicted in this way, assuming the earlier values of $Z_0 = 50\ \Omega$, $d = 0.2$ m, $\varepsilon_r = 2.3$, $L = 115$ nH, $C_S = 45$ pF, and $\alpha = 0.6$.

The qualitative agreement between experiment and theory is clearly reasonable, and the locations and widths of the two bands are correctly predicted using parameter values estimated from entirely separate experiments. A reduction in the measured transmission can be attributed to losses, as can any propagation outside the bands, while oscillations in transmission can be attributed to etalon effects.

V. Conclusion

An analysis of transmission lines that are periodically interrupted by isolation transformers has been carried out. The dispersion characteristics have been derived, and it has been shown that the arrangement supports MI waves propagating in bands lying close to the resonant frequencies of short-circuited line segments. Additional series capacitors allow operation at lower frequencies via a further lumped-element MI band. Experiments have been carried out using resonant elements constructed from coaxial cable and PCB inductors. The results confirm the existence of a set of propagating bands and the independent adjustment of a low-frequency band using capacitors, and good agreement is obtained between experiment and theory.

Such lines already have practical application as safe interconnects to an RF detector in internal MRI, where continuous lines may be heated by resonant excitation. This application demonstrates that metamaterials can have an important role in signal propagation over short distances, where useful properties such as bandpass characteristics can overcome disadvantages such as relatively high propagation loss. However, since transformer-coupled lines effectively separate out the two functions of magnetic coupling and propagation, very high coupling can be employed without reducing the interelement spacing that occurs in a purely lumped-element system. Consequently, other applications may exist where lowloss MI wave propagation may be required over larger physical distances. The use of flexible cabling also offers a simple method of propagating an MI wave round a bend without reflection from line discontinuities.

References

[1] L. Brillouin, *Wave Propagation in Periodic Structures: Electric Filters and Crystal Lattices*, 2nd ed. New York: Dover, 1953.

[2] R. A. Silin and V. P. Sazonov, *Slow Wave Structures*. Boston Spa, U.K.: National Lending Library for Science and Technology, 1971.

[3] V. G. Veselago, "The electrodynamics of substances with simultaneously negative values of ε and μ," *Sov. Phys. Usp.*, vol. 10, pp. 509–514, Jan./Feb. 1968.

[4] J. B. Pendry, A. J. Holden, D. J. Robbins, and W. J. Stewart, "Magnetism from conductors and enhanced nonlinear phenomena," *IEEE Trans. Microw. Theory Tech.*, vol. MTT-47, no. 11, pp. 2075–2084, Nov. 1999.

[5] D. R. Smith, W. J. Padilla, D. C. Vier, S. C. Nemat-Nasser, and S. Schultz, "Composite medium with simultaneously negative permeability and permittivity," *Phys. Rev. Lett.*, vol. 84, pp. 4184–4187, May 2000.

[6] N. Engheta and R. W. Ziolkowski, *Metamaterials*. New York: Wiley, 2006.

[7] L. Solymar and E. Shamonina, *Waves in Metamaterials*. Oxford, U.K.: Oxford Univ. Press, 2009.

[8] M. K. Konings, L. W. Bartels, H. F. M. Smits, and C. J. G. Bakker, "Heating around intravascular guidewires by resonating RF waves," *J. Mag. Reson. Imaging*, vol. 12, pp. 79–95, Jul. 2000.

[9] W. R. Nitz, A. Oppelt, W. Renz, C. Manke, M. Lenhart, and J. Link, "On the heating of linear conductive structures as guidewires and catheters in interventional MRI," *J. Mag. Reson. Imaging*, vol. 13, pp. 105–114, Jan. 2001.

[10] A. Surowiec, S. S. Stuchly, L. Eidus, and A. Swarup, "In-vitro dielectric properties of human tissue at radio frequencies," *Phys. Med. Biol.*, vol. 32, pp. 615–621, May 1987.

[11] E. Atalar, "Safe coaxial cables," in *Proc. 7th Ann. Meeting ISMRM*, Philadelphia, PA, 1999, p. 1006.

[12] M. E. Ladd and H. H. Quick, "Reduction of resonant RF heating in intravascular catheters using coaxial chokes," *Mag. Reson. Med.*, vol. 43, pp. 615–619, Apr. 2000.

[13] S. Weiss, P. Vernickel, T. Schaeffter, V. Schulz, and B. Gleich, "Transmission line for improved RF safety of interventional devices," *Mag. Reson. Med.*, vol. 54, pp. 182–189, Jun. 2005.

[14] P. Vernickel, V. Schulz, S. Weiss, and B. Gleich, "A safe transmission line for MRI," *IEEE Trans. Biomed. Eng.*, vol. 52, no. 6, pp. 1094–1102, Jun. 2005.

[15] A. Krafft, S. Müller, R. Umathum, W. Semmler, and M. Bock, "B_1 field-insensitive transformers for RF-safe transmission lines," *Mag. Reson. Mater. Phys.*, vol. 19, pp. 257–266, Nov. 2006.

[16] C. Caloz and T. Itoh, "Application of the transmission line theory of left-handed (LH) materials to the realization of a microstrip "LH line"," in *Proc. IEEE-APS Int. Symp. Dig.*, Jun. 2002, vol. 2, pp. 412–415.

[17] A. Sanada, C. Caloz, and T. Itoh, "Characteristics of the composite right/left-handed transmission lines," *IEEE Microw. Wireless Compon. Lett.*, vol. 14, no. 2, pp. 68–70, Feb. 2004.

[18] C. Caloz and T. Itoh, *Electromagnetic Metamaterials: Transmission Line Theory and Microwave Applications*. Hoboken, NJ: Wiley, 2006.

[19] G. V. Eleftheriades, A. K. Iyer, and P. C. Kremer, "Planar negative refractive index media using periodically L-C loaded transmission lines," *IEEE Trans. Microw. Theory Tech.*, vol. 50, no. 12, pp. 2702–2712, Dec. 2002.

[20] G. V. Eleftheriades, O. Siddiqui, and A. K. Iyer, "Transmission line models for negative refractive index media and associated implementations without excess resonators," *IEEE Microw. Wireless Compon. Lett.*, vol. 13, no. 2, pp. 51–53, Feb. 2003.

[21] A. Grbic and G. V. Eleftheriades, "Periodic analysis of a 2-D negative refractive index transmission line structure," *IEEE Trans. Antennas Propag.*, vol. 51, no. 10, pp. 2604–2611, Oct. 2003.

[22] E. Shamonina, V. A. Kalinin, K. H. Ringhofer, and L. Solymar, "Magneto-inductive waveguide," *Electron. Lett.*, vol. 38, no. 8, pp. 371–373, Apr. 2002.

[23] M. C. K. Wiltshire, E. Shamonina, I. R. Young, and L. Solymar, "Dispersion characteristics of magneto-inductive waves: Comparison between theory and experiment," *Electron. Lett.*, vol. 39, no. 2, pp. 215–217, Jan. 2003.

[24] R. R. A. Syms, I. R. Young, and L. Solymar, "Low-loss magneto-inductive waveguides," *J. Phys. D, Appl. Phys.*, vol. 39, pp. 3945–3951, Sep. 2006.

[25] S. Maslovski, P. Ikonen, I. Kolmakov, and S. Tretyakov, "Artificial magnetic materials based on the new magnetic particle: Metasolenoid," *Progress Electromagn. Res.*, vol. 54, pp. 61–81, 2005.

[26] L. Jylhä, S. Maslovski, and S. Tretyakov, "Traveling waves along the metasolenoid," in *Proc. PIER Symp.,* Mar. 2009, Cambridge, MA, p. 456.

[27] M. C. K. Wiltshire, E. Shamonina, I. R. Young, and L. Solymar, "Experimental and theoretical study of magneto-inductive waves supported by one-dimensional arrays of 'Swiss Rolls'," *J. Appl. Phys.*, vol. 95, pp. 4488–4493, Apr. 2004.

[28] M. J. Freire, R. Marques, F. Medina, M. A. G. Laso, and F. Martin, "Planar magneto-inductive wave transducers: Theory and applications," *Appl. Phys. Lett.*, vol. 85, pp. 4439–4441, Nov. 2004.

[29] I. S. Nefedov and S. A. Tretyakov, "On potential applications of metamaterials for the design of broadband phase shifters," *Microw. Opt. Technol. Lett.*, vol. 45, no. 2, pp. 98–102, Apr. 2005.

[30] M. J. Freire and R. Marques, "Planar magnetoinductive lens for three-dimensional subwavelength imaging," *Appl. Phys. Lett.*, vol. 86, pp. 182505-1–182505-3, Apr. 2005.

[31] O. Sydoruk, M. Shamonin, A. Radkovskaya, O. Zhuromskyy, E. Shamonona, R. Trautner, C. J. Stevens, G. Faulkner, D. J. Edwards, and L. Solymar, "Mechanism of subwavelength imaging with bilayered

magnetic metamaterials: Theory and experiment," *J. Appl. Phys.*, vol. 101, pp. 073903-1–073903-8, Apr. 2007.
[32] M. C. K. Wiltshire, J. B. Pendry, I. R. Young, D. J. Larkman, D. J. Gilderdale, and J. V. Hajnal, "Microstructured magnetic materials for RF flux guides in magnetic resonance imaging," *Science*, vol. 291, pp. 849–851, Feb. 2001.
[33] E. Shaminona and L. Solymar, "Properties of magnetically coupled metamaterial elements," *J. Magn. Magn. Mater.*, vol. 300, pp. 38–43, Jan. 2006.
[34] E. Shamonina and L. Solymar, "Slow waves in magnetic metamaterials: History, fundamentals and applications," *Phys. Stat. Sol. B*, vol. 245, pp. 1471–1482, Jun. 2008.
[35] R. R. A. Syms, L. Solymar, and I. R. Young, "MR-safe cables—An application of magneto-inductive waves?," presented at the 3rd Int. Congr. Adv. Electromagn. Mater. Microw. Opt., London, U.K., Aug. 30–Sep. 4, 2009..

Richard R. A. Syms (SM'02) received the B.A. and D.Phil. degrees from Oxford University, Oxford, U.K., in 1979 and 1982, respectively.

He was an Atlas Research Fellow with Rutherford Appleton Laboratory, Didcot, Oxon, U.K. He was a Reader, a Senior Lecturer, and a Senior Research Fellow at Imperial College London, London, U.K., where he is currently a Professor of microsystems technology in the Department of Electrical and Electronic Engineering, and leads the Optical and Semiconductor Devices Group. He is the author or coauthor of more than 200 journals and conference papers published in the field of volume holography, guided wave optics, electromagnetic theory, microelectromechanical systems, and metamaterials. His research interests include the development of improved detection systems for MRI.

Prof. Syms is a Fellow of the Royal Academy of Engineering, the Institute of Electrical Engineers, and the Institute of Physics.

Laszlo Solymar received the B.Sc. degree from Technical University of Budapest, Hungary, in 1952 and the Ph.D. degree from Hungarian Academy of Sciences, in 1956.

He was with Standard Telecommunications Laboratories, Essex, U.K., for many years. He was a Professor of applied electromagnetism in the Department of Engineering Science, Oxford University, Oxford, U.K. He is currently a Senior Research Fellow and a Visiting Professor in the Department of Electrical and Electronic Engineering, Imperial College London, London, U.K. He has published extensively in the fields of communications, electromagnetic theory, photorefractive materials, volume holography, superconductivity, traveling wave electron devices and antenna arrays, as well as many books on similar topics. His research interests include RF metamaterials and traveling wave amplifiers for terahertz frequencies.

Prof. Solymar is a Fellow of the Royal Society and the Institute of Electrical Engineers.

Ian R. Young received the B.Sc. and Ph.D. degrees from the University of Aberdeen, Aberdeen, U.K., in 1954 and 1958, respectively.

He was the Vice President (Research) of Picker International. From its foundation until 1997, he was with Hammersmith Hospital, London, U.K., where he led the Physics and Engineering Group in the Robert Steiner MRI Unit. He is currently a Senior Research Fellow and a Visiting Professor in the Department of Electrical and Electronic Engineering, Imperial College London, London, U.K. He is the author or coauthor of more than 300 papers published in the field related to the development of MRI and MRS. He is the holder of 50 patents. His research interests include the development of *in vivo* MRI systems and MR-guided surgical robots.

Mr. Young is a Fellow of the Royal Society and the Royal Academy of Engineering. He was the recipient of the Gold Medal of the Society of Magnetic Resonance in Medicine (SMRM), the Silver Medal of the International Society of Magnetic Resonance in Medicine (ISMRM), the Duddell Medal (Institute of Physics), and the Sir Frank Whittle Prize (Royal Academy of Engineering). He was the President of SMRM during 1991–1992, and the Secretary of ISMRM during 1993–1996.